Control of an Over-Actuated Single-Degree-of-Freedom Excitation System

Michael T. Hale, United States Army Redstone Test Center, Dynamic Test Division
Norman Fitz-Coy, Dept. of Mechanical and Aerospace Engineering, University of Florida

Abstract

This paper provides results of a laboratory experiment designed to illustrate the theoretical control considerations for an over-actuated excitation system. The experiment is based on control of a beam pinned at one end providing a single rotational degree of freedom and excited by two electrodynamic actuators. Control is achieved through implementation of two different control reference techniques: (1) reference based on linear acceleration autospectral densities (ASD) and cross-spectral densities (CSD) using linear accelerometer feedback and (2) reference based on an angular acceleration ASD using estimates of angular acceleration as feedback. Correlations to the theoretical based predictions were conducted based on common measurements of both linear acceleration and estimates of angular acceleration acquired during each trial.

KEYWORDS

Over-actuated, multiple exciter test, pseudo inverse, spectral density matrix, single degree of freedom, autospectral density, cross-spectral density

BACKGROUND

The most common laboratory vibration test consists of a single exciter providing motion in a single mechanical degree of freedom (DOF). However, there are many circumstances that will require use of multiple exciters to meet test objectives. A multiple exciter test (MET) is required whenever more than one mechanical degree of freedom is required simultaneously, when a single actuator is not capable of addressing the test requirement, or possibly a combination of both scenarios. Clearly, one could envision unlimited combinations of actuator placements, actuator performance, and payload factors. Of particular interest, and the subject of this study, is the over-actuated MET case. An excitation system is considered to be over-actuated whenever the number of actuators exceeds the number of motion degrees of freedom. A comprehensive discussion of the primary challenges associated with controlling over-actuated systems ranging from a single mechanical degree of freedom through six degree-of-freedom scenarios are discussed in detail in reference 1. This study will illustrate the ideas presented in reference 1 through a practical, laboratory-based experiment.

EXPERIMENT DESCRIPTION

The objective of the experiment is to control two electrodynamic actuators driving a fixture (also referred to as the platform or body P) that is pinned at one end, providing a single rotational degree of freedom. Configuring the laboratory experiment in the form of a simple 1-DOF over-actuated MET makes implementation of the ideas presented in reference 1 straightforward to apply and interpret. The test system layout is shown in Figure 1. Observe that vectors $\underline{l}_1$ and $\underline{l}_2$ define the position relative to the center of rotation, position o in Figure 1, to which the actuators are attached to the beam. Similarly, vectors $\underline{r}_1$ and $\underline{r}_2$ define the position of the control accelerometers. Although it is not required, the control accelerometers and actuator attachment points were collocated for the experiment being discussed.

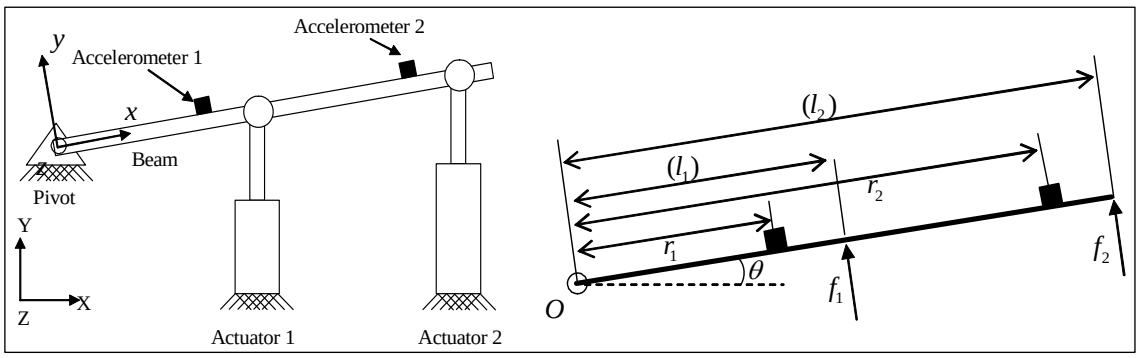

Figure 1. Illustration of over-actuated MET to obtain 1-DOF angular motion (rotation about the z-axis).

The simple beam serving as the test fixture was designed to have a bending mode within the test bandwidth of interest. Clearly, one would generally avoid purposely placing a mode within the test bandwidth; however, it is commonly necessary to contend with undesirable modes that reside within the test bandwidth of interest, particularly as the excitation system increases in size. Through the use of a basic finite-element model, estimates of significant modes were predicted at approximately 320 and 500 Hz for the example being considered.

Two control strategies were considered for the experiment. The first method was a spectral-based control scheme in which the reference was defined in terms of autospectral densities (ASDs) and cross-spectral densities (CSDs) in Engineering Units (EUs) of linear acceleration. For the purpose of this discussion, the first control technique will be referred to as *square control*. The second control method was based on I/O transformations[2] and the reference was defined as a single ASD in EUs of angular acceleration. The second control technique will be referred to as I/O *transform control*.

Square Control Test Parameters

A spectral density matrix of the form shown in equation 1 is required to define the reference criteria for the square control case. Most modern vibration control systems will also accept the CSD terms in terms of relative phase and coherence.

$$\begin{bmatrix} ASD(f)_{y1y1} & CSD^*(f)_{y1y2} \\ CSD(f)_{y1y2} & ASD(f)_{y2y2} \end{bmatrix} \quad (1)$$

For the system illustrated in Figure 1, the optimal phase relationship between the two actuators would be 0 degrees and the coherence would be 1.0. Otherwise, extreme forces would be imparted on the fixture and associated couplings as well as a significant performance reduction for the motion degree of freedom desired (rotation about the z-axis for this example). Unfortunately, if the phase and coherence were set to 0 and 1.0 respectively, the spectral density matrix would be rank-deficient.[2] However, setting the phase relationship to 0 degrees and the coherence to approximately 0.95 will result in a minor difference between the reference signals and generally should be sufficient to avoid the issue of rank deficiency. The relationship between the ASD terms can be defined in terms of the input transform,[1] which is defined as the relationship between the measurement space (i.e., accelerometer outputs) and the motion space (i.e., physical motion of the platform). In reference 1, the relationship between the measurement space and physical space for the rigid body case is defined as:

$$a_{k_j} = \begin{bmatrix} \underline{e}_j^T & -\underline{e}_j^T \left[{}^P\underline{r}_i^P \right]^\times \end{bmatrix} \begin{bmatrix} {}^P\underline{a}_o^P \\ {}^P\underline{\alpha}^P \end{bmatrix} \tag{2}$$

where $k \in (1, 2, ..., n)$, $i \in (1, 2, ..., n^*)$ and $j \in (x, y, z)$. Parameter n represents the number of accelerometer measurements and n^* is an index defining the measurement location. Observe that if multi-axis accelerometers are employed, then $n^* < n$. Parameters $\underline{e}_x^T = [1 \quad 0 \quad 0]$, $\underline{e}_y^T = [0 \quad 1 \quad 0]$, and $\underline{e}_z^T = [0 \quad 0 \quad 1]$ are defined as row selection matrices and $\left[{}^P\underline{r}_i^P \right]^\times$ is the skew symmetric operator equivalent of the cross-product. As in reference 1, the matrix equivalent of a vector (i.e., a coordinatized vector quantity) is denoted as ${}^{(\,)}(\_)^{(\,)}_{(\,)}$ where the right superscript and subscript identify the body and point of interest, respectively, and the left superscript denotes the coordinate frame in which the vector quantity was coordinatized; e.g., ${}^P\underline{r}_i^P$ in equation 2 denotes the *i* th point on body P (the platform) coordinatized in frame $\mathcal{F}_P$.

For the 1-DOF example considered in Figure 1, two accelerometers placed incident to the actuator attachment points were employed as the control accelerometers. From equation 1, the input transformation can be established.

$$a_{1y} = \begin{bmatrix} 0,1,0,(0,-1,0) \begin{pmatrix} 0 & -r_{1z} & r_{1y} \\ r_{1z} & 0 & -r_{1x} \\ -r_{1y} & r_{1x} & 0 \end{pmatrix} \end{bmatrix} \begin{bmatrix} a_{0x} \\ a_{0y} \\ a_{0z} \\ \alpha_x \\ \alpha_y \\ \alpha_z \end{bmatrix} = [0,1,0,-r_{1z},0,r_{1x}] \begin{bmatrix} a_{0x} \\ a_{0y} \\ a_{0z} \\ \alpha_x \\ \alpha_y \\ \alpha_z \end{bmatrix} \tag{3}$$

$$a_{2y} = \begin{bmatrix} 0,1,0,(0,-1,0) \begin{pmatrix} 0 & -r_{2z} & r_{2y} \\ r_{2z} & 0 & -r_{2x} \\ -r_{2y} & r_{2x} & 0 \end{pmatrix} \end{bmatrix} \begin{bmatrix} a_{0x} \\ a_{0y} \\ a_{0z} \\ \alpha_x \\ \alpha_y \\ \alpha_z \end{bmatrix} = [0,1,0,-r_{2z},0,r_{2x}] \begin{bmatrix} a_{0x} \\ a_{0y} \\ a_{0z} \\ \alpha_x \\ \alpha_y \\ \alpha_z \end{bmatrix} \tag{4}$$

For the laboratory experiment being considered, the locations of the control accelerometers are defined in EUs of inches using a Cartesian coordinate system as defined in Figure 1, i.e., $r_1^T = [9 \quad 0 \quad 0]$ and $r_2^T = [21 \quad 0 \quad 0]$. By having the platform pinned as shown in Figure 1, translational motion and angular motion about the x and y axes have been constrained, simplifying equations 3 and 4 as shown in equation 5. Observe that equation 5 is of the form $A_{meas} = \bar{I}A_{motion}$.

$$\begin{bmatrix} a_{1y} \\ a_{2y} \end{bmatrix} = \begin{bmatrix} 0 & 1 & 0 & 0 & 0 & 9 \\ 0 & 1 & 0 & 0 & 0 & 21 \end{bmatrix} \begin{bmatrix} 0 \\ 0 \\ 0 \\ 0 \\ 0 \\ \alpha_z \end{bmatrix} = \begin{bmatrix} 9 \\ 21 \end{bmatrix} \alpha_z \tag{5}$$

Although equation 5 for the 1-DOF example being considered is of a simple construct in which α_z could be readily solved, the requirements for solving for the general case still apply. Specifically, if $\bar{I}$ is of full column rank, then $\left[\bar{I}^T\bar{I}\right]^{-1}$ exists, enabling A_{motion} to be solved as follows:

$$\begin{aligned} A_{Meas} &= \bar{I}A_{Motion} \\ \bar{I}^T A_{Meas} &= \bar{I}^T\bar{I}A_{Mot} \\ \left[\bar{I}^T\bar{I}\right]^{-1}\bar{I}^T A_{Meas} &= \left[\bar{I}^T\bar{I}\right]^{-1}\bar{I}^T\bar{I}A_{Mot} \\ \left[\bar{I}^T\bar{I}\right]^{-1}\bar{I}^T A_{Meas} &= A_{Mot} \end{aligned} \tag{6}$$

For the example being considered, the aforementioned calculation yields:

$$\begin{bmatrix} .0172 & .0402 \end{bmatrix} \begin{bmatrix} a_{1y} \\ a_{2y} \end{bmatrix} = \alpha_z \tag{7}$$

Having resolved the linear relationship between acceleration at accelerometer locations 1 and 2, it is possible to develop the relationship between reference ASDs for the square control case. For the specific example being considered, $ASD(f)_{y1y1} = (.0172/.0402)^2\, ASD(f)_{y2y2}$. For the example at hand, the ASD reference criteria at position $\underline{r}_2 = \begin{bmatrix} 21 & 0 & 0 \end{bmatrix}^T$ was arbitrarily defined as $0.010\ g^2/Hz$ over the bandwidth of 10–500 Hz and thereby establishing the ASD reference at position $\underline{r}_1 = \begin{bmatrix} 9 & 0 & 0 \end{bmatrix}^T$ as $(0.0172/0.0402)^2$ *0.01=0.0018 g^2/Hz over the same bandwidth of 10–500 Hz. Figure 2 illustrates the quality of control at accelerometer locations 1 and 2.

Figure 2. Square control.

Recall that the control accelerometers for this example were collocated with the actuator-to-fixture interface. If no other measurement transducers were included, the undesired spectral response associated with the modes anticipated at 320 and 500 Hz would have been missed entirely, leaving the impression that any test item residing on the platform had been exposed to a pure rotational motion. Through inclusion of two additional accelerometers sensing acceleration in the y-axis at positions $[15 \quad 0 \quad 0]$ and $[23.5 \quad 0 \quad 0]$, Figure 3 illustrates the effects of in-band test modes as predicted pre-test by the finite element model. Figure 3 also illustrates why great care should be taken with the assumption of rigid body motion when using linear accelerometers to predict angular motion.

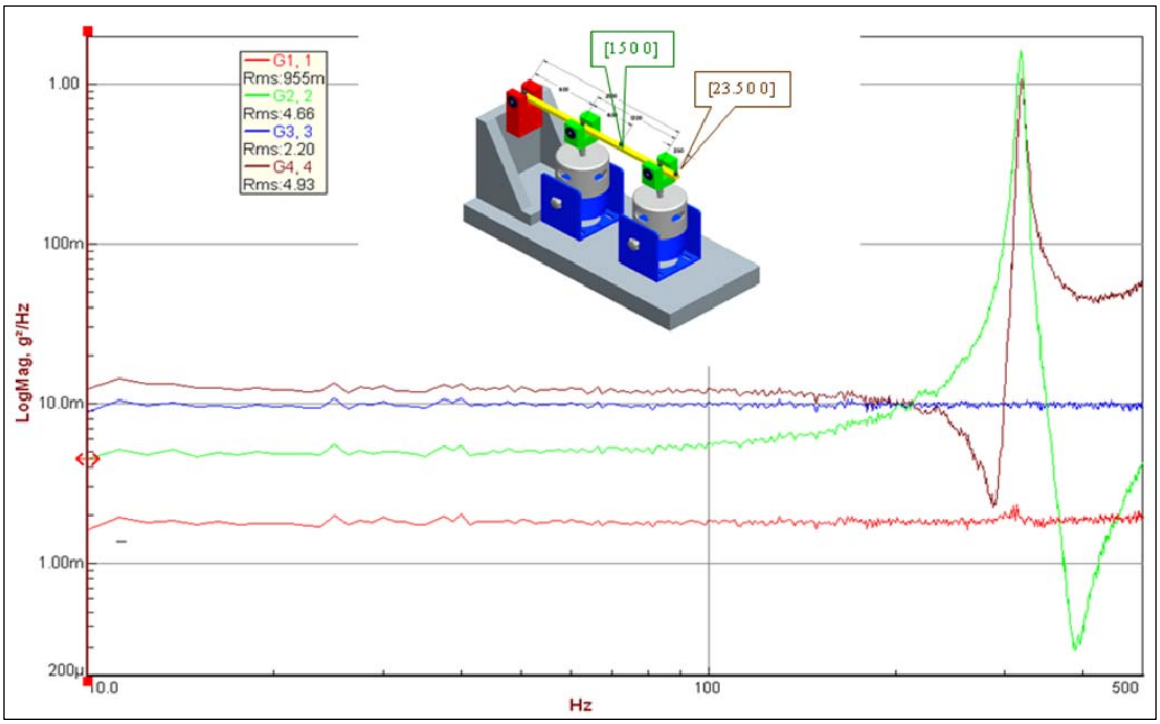

Figure 3. Square control with Y-axis ASD measurements at positions [15 0 0] and [23.5 0 0].

I/O Transformation Test Parameters

The reference for I/O transformation based control of the 1-DOF example being considered is simply an ASD in EUs of angular acceleration. The input transformation has already been discussed in the previous section. Specifically, using equation 5, the two linear accelerometers at positions $r_1 = [9 \quad 0 \quad 0]$ and $r_2 = [21 \quad 0 \quad 0]$ are used to estimate the angular acceleration about the z-axis as:

$$\alpha_z = \frac{(a_{2y} - a_{1y})}{(21-9)} \tag{8}$$

This operation is represented by Block A in Figure 4. To be consistent with the square control example shown in the previous section, the reference ASD is defined as $3.43\ (\text{rad/s}^2)^2/\text{Hz}$ over a bandwidth of 10–500 Hz. This ASD reference, which is in EU of angular acceleration, is readily computed from equation 8 by considering the g-rms levels of each of the two control accelerometers used in the square control case. Having established the rms level in EU of $(\text{rad/s}^2)_{\text{rms}}$ combined with knowledge of the bandwidth and spectral shape, the magnitude of the ASD can be computed. Since I/O transform control is based on ASD and CSD relationships of the six traditional motion degrees of freedom[2] and the example at hand is a 1-DOF scenario, there will be no CSD terms in defining the reference criteria.

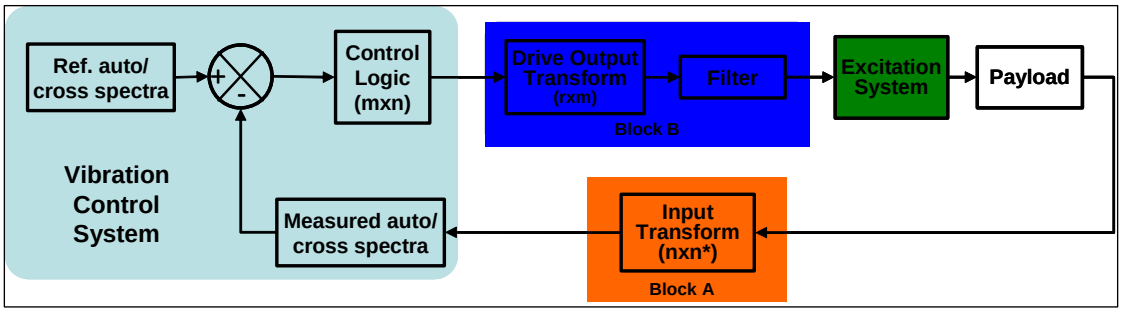

Figure 4. Block diagram for I/O transform control.

Having defined the structure of the input transformation and the reference ASD, the only remaining activity in preparing for the I/O transform control for the example at hand is to define the output transform. While the input transformation was based on transducer locations, the output transform will be structured on the basis of the position and orientation of the actuators. In reference 1, the output transform is represented by the P-Matrix (Plucker Matrix),[1,3,4] as defined in equation 9.

$$\underset{6xd}{P}\;\underset{dx1}{F}=\underset{6x1}{C}$$

$$\begin{bmatrix} {}^{B}\underline{\hat{u}}_1 & {}^{B}\underline{\hat{u}}_2 & \cdots & {}^{B}\underline{\hat{u}}_d \\ {}^{P}\underline{m}_1^{P} & {}^{P}\underline{m}_2^{P} & \cdots & {}^{P}\underline{m}_d^{P} \end{bmatrix}\begin{bmatrix} f_1 \\ f_2 \\ \vdots \\ f_d \end{bmatrix}=\begin{bmatrix} m\left({}^{B}\underline{a}_C^{P}-{}^{B}\underline{g}\right)-{}^{B}\underline{F}_E \\ {}^{P}\underline{\underline{I}}_C^{P}\,{}^{P}\underline{\dot{\omega}}^{P}+\left[{}^{P}\underline{\omega}^{P}\right]^{\times}{}^{P}\underline{\underline{I}}_C^{P}\left({}^{P}\underline{\omega}^{P}\right)-{}^{P}\underline{M}_E \end{bmatrix} \tag{9}$$

The variables ${}^{B}\underline{\hat{u}}_i$ represent the Line of Action (LOA) vectors for each of the actuators and ${}^{P}\underline{m}_i^{P}$ is the moment arm associated with force f_i. Matrix $\underline{\underline{L}}_{PB}$ is the direction cosine transformation matrix employed to coordinatize ${}^{B}\underline{\hat{u}}_i$ from the base coordinate frame, $\mathcal{F}_B$, into the platform frame, $\mathcal{F}_P$. For the two-actuator example at hand, there are no translational motion degrees-of-freedom, leaving only ${}^{P}\underline{m}_1^{P}$ and ${}^{P}\underline{m}_2^{P}$ to formulate the P matrix. As shown in reference 1, the column matrix is obtained from the skew-matrix equivalent of the vector cross-product as:

$${}^{P}\underline{m}_i^{P}=\left[{}^{P}\underline{r}_i^{P}\right]^{\times}\underline{\underline{L}}_{PB}\,{}^{B}\underline{\hat{u}}_i=\begin{bmatrix} 0 & -z_i^{P} & y_i^{P} \\ z_i^{P} & 0 & -x_i^{P} \\ -y_i^{P} & x_i^{P} & 0 \end{bmatrix}\underline{\underline{L}}_{PB}\,{}^{B}\underline{\hat{u}}_i \tag{10}$$

For the example at hand, the angular motion is < 10 degrees, thus, ${}^{P}\underline{m}_i^{P}\;i=1,2$ is closely approximated as:

$${}^{P}m_1^{P}=\left[\left[{}^{P}r_1^{P}\right]^{x}\underline{\underline{L}}_{PB}\,{}^{B}\hat{u}_1\right]=\begin{bmatrix} 0 & 0 & 0 \\ 0 & 0 & -9 \\ 0 & 9 & 0 \end{bmatrix}\begin{bmatrix} \cos\theta & \sin\theta & 0 \\ -\sin\theta & \cos\theta & 0 \\ 0 & 0 & 1 \end{bmatrix}\begin{bmatrix} 0 \\ 1 \\ 0 \end{bmatrix}=\begin{bmatrix} 0 \\ 0 \\ 9\cos\theta \end{bmatrix}\cong\begin{bmatrix} 0 \\ 0 \\ 9 \end{bmatrix}$$

$${}^{P}m_2^{P}=\left[\left[{}^{P}r_2^{P}\right]^{x}\underline{\underline{L}}_{PB}\,{}^{B}\hat{u}_2\right]=\begin{bmatrix} 0 & 0 & 0 \\ 0 & 0 & -21 \\ 0 & 21 & 0 \end{bmatrix}\begin{bmatrix} \cos\theta & \sin\theta & 0 \\ -\sin\theta & \cos\theta & 0 \\ 0 & 0 & 1 \end{bmatrix}\begin{bmatrix} 0 \\ 1 \\ 0 \end{bmatrix}=\begin{bmatrix} 0 \\ 0 \\ 21\cos\theta \end{bmatrix}\cong\begin{bmatrix} 0 \\ 0 \\ 21 \end{bmatrix}$$

Acknowledging the constrained mechanical DOFs, this can be written in the form of equation 9 as:

$$\begin{bmatrix} 0 & 0 \\ 0 & 0 \\ 0 & 0 \\ 0 & 0 \\ 0 & 0 \\ 9 & 21 \end{bmatrix} \begin{bmatrix} f_1 \\ f_2 \end{bmatrix} = \begin{bmatrix} 0 \\ 0 \\ 0 \\ 0 \\ 0 \\ c_6 \end{bmatrix} \quad \rightarrow \quad \underset{P}{\begin{bmatrix} 9 & 21 \end{bmatrix}} \underset{F}{\begin{bmatrix} f_1 \\ f_2 \end{bmatrix}} = \underset{C}{c_6} \tag{11}$$

Next, the objective is to solve for F. Recall that I/O transform control of the problem at hand is based on a single feedback signal in EU of angular acceleration and a single reference ASD, yielding a single drive signal, D. Our mechanical system, however, consists of two actuators. As discussed in reference 1, defining $F \equiv P^T D$ and substituting into $PF = C$ yields $PP^T D = C$. As long as P is of full row rank, $\left[PP^T \right]^{-1}$ exists,[1] in which case $D = \left[PP^T \right]^{-1} C$. Thus, for the example at hand, as formulated in equation 12,

$$\underset{2x1}{F} \equiv \underset{2x1}{P^T} \underset{1x1}{D} = \underset{2x1}{P^T} \left[\underset{1x2}{P} \underset{2x1}{P^T} \right]^{-1} \underset{1x1}{C} = \begin{bmatrix} 9 \\ 21 \end{bmatrix} \left[\begin{bmatrix} 9 & 21 \end{bmatrix} \begin{bmatrix} 9 \\ 21 \end{bmatrix} \right]^{-1} C = \begin{bmatrix} .0172 \\ .0402 \end{bmatrix} C \tag{12}$$

$$\begin{bmatrix} f_1 \\ f_2 \end{bmatrix} = \begin{bmatrix} .0172 \\ .0402 \end{bmatrix} C \quad \Rightarrow \quad f_1 = .4278 f_2$$

The relationship $f_1 = .4278 f_2$ is then captured in Block B of Figure 4. Observe that the relationship between drive signals is based purely on magnitude. This implies that the actuators, including associated power supplies and instrumentation, must be matched systems. This is a weakness of the I/O transform in the form shown. The filter block within Block B is a placeholder for future research into accounting for mismatched systems. Figure 5 illustrates the results of the I/O transform-based control of the example at hand.

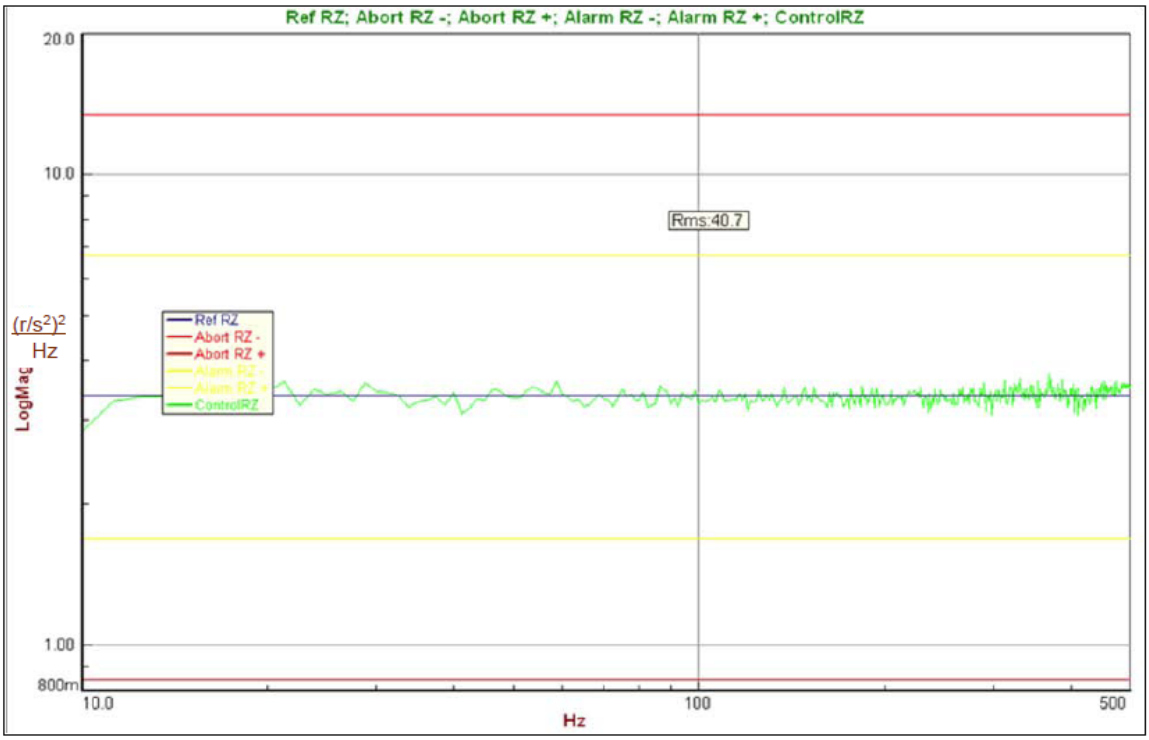

Figure 5. I/O transform control.

As was the case for the square control example discussed earlier, if no other measurement transducers were included, the undesired spectral response associated with the modes anticipated at 320 and 500 Hz would have been missed entirely, leaving the impression that any test item residing on the platform had been exposed to a pure rotational motion. Through inclusion of the same two additional accelerometers that were considered when discussing the square control results, Figure 6 illustrates the effects of in-band test modes as predicted pre-test by finite element model. Figure 6 also shows the linear accelerometer measurements that were used as control points for the square control case.

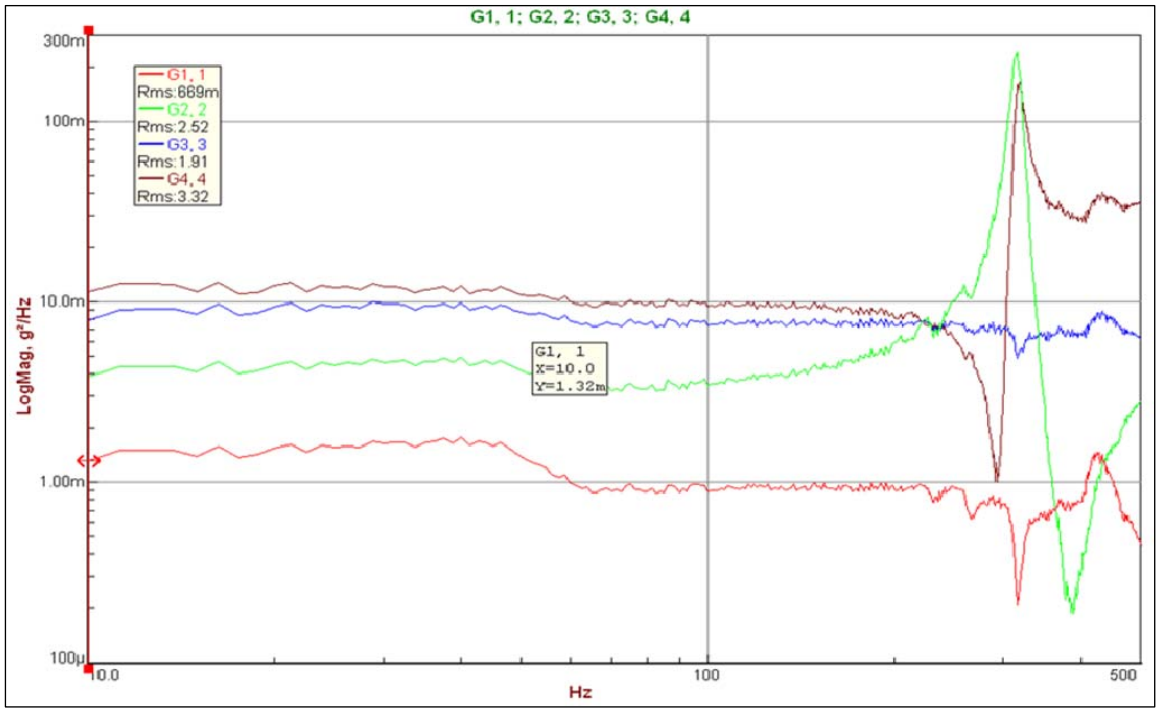

Figure 6. Y-axis linear ASD measurements acquired during I/O transform control.

Observe that the blue and red curves representing the accelerometers at actuator positions $r_1 = [9 \quad 0 \quad 0]$ and $r_2 = [21 \quad 0 \quad 0]$, respectively, are not perfectly flat as they were for the square control case. This is a result of the actuators not being perfectly matched and effects of the modal characteristics of the first mode at 320 Hz. Issues with the anticipated modes are still evident and similar to that of the square control case illustrated in Figure 3. With the exception of the spectral band in the vicinity of the undesirable mode at 320 Hz, the differences between the linear accelerometers coincident with actuators 1 and 2 are very similar in shape to the known mismatch in actuators that was estimated prior to running the I/O transform-based control. The estimate was made by controlling both actuators to a common spectra (with the platform removed) and observing the transfer function between the drive signals, as shown in Figure 7.

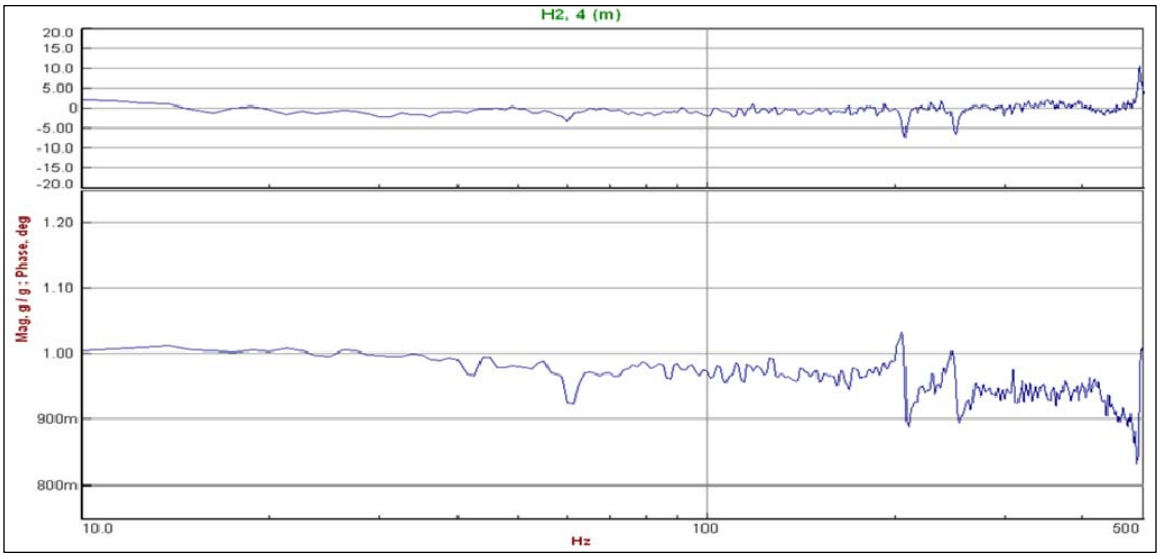

Figure 7. Illustration of the degree of similarity between actuation systems.

Note that it is not possible to eliminate the undesired in-band modes without inclusion of additional actuators or possibly by redesigning the platform. However, it is still possible, as in traditional Single-Exciter/Single-Actuator (SESA)[5] control, to limit or notch undesired response as illustrated in Figure 8. As always, when employing limiting strategies, one should verify that limiting strategies will not compromise the integrity of the test and document the process thoroughly. Similar results were obtained when employing the same notching criteria for the square control case.

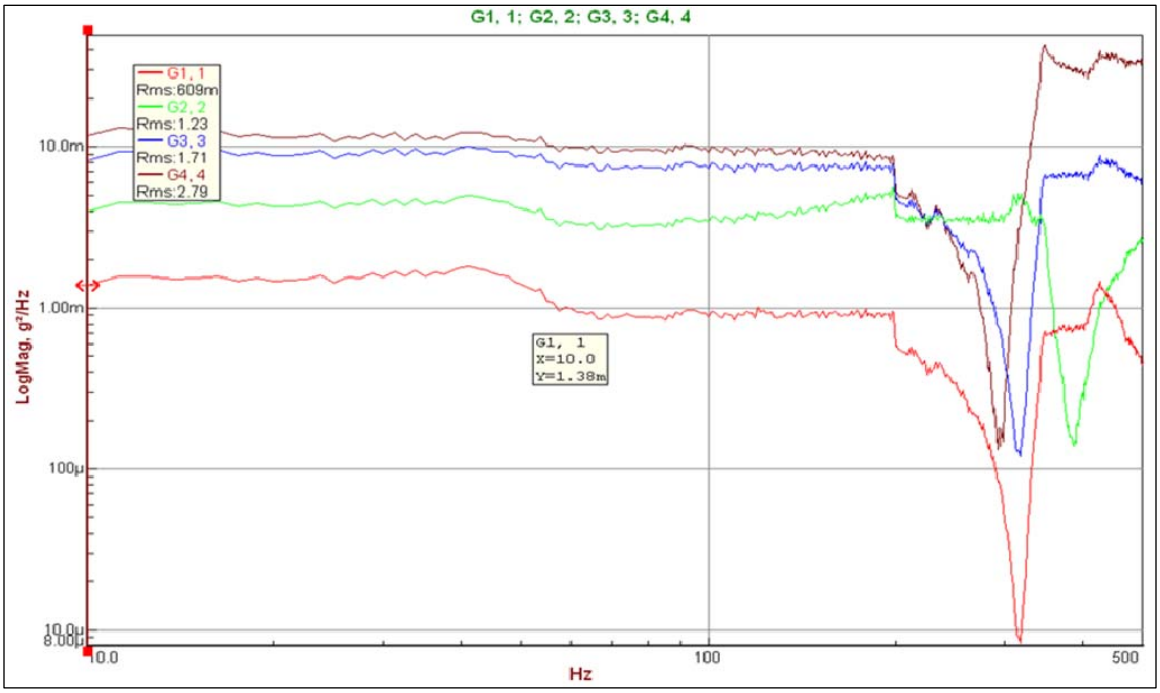

Figure 8. Y-axis linear ASD measurements acquired during I/O transform control with measurement position [15 0 0] configured as a notching channel.

CONCLUSIONS

A 1-DOF laboratory-based physical example of an over-actuated system was considered to illustrate the generalized process discussed in reference 1. The generalized process for documenting input and output transformation characteristics was illustrated through an example for which all computations were readily performed by hand, while demonstrating the scalability of the process to much more complex systems. Even the simple example employed clearly illustrated the critical need to understand both system kinematics and instrumentation requirements associated with MET. The importance of modeling a MET system was also illustrated to ensure that any undesired modal characteristics are understood and that a plan is in place to employ notching strategies if required.

Mechanical constraints must be well understood, and in the case of servo-hydraulic actuators, compliance characteristics must also be understood. If not properly addressed by either passive or active measures, unmatched servo-hydraulic actuators employed in a MET configuration could result in significant undesired stress levels on the actuation system or possibly the test article, depending upon how the system is configured.[1]

Both square and I/O transform-based control proved to be effective. The effects of the actuators not being perfectly matched are more evident in the I/O transform scenario. Further research is recommended to address the issues associated with mismatched actuation systems for the MET scenario.

REFERENCES

1. Fitz-Coy, N., V. Nagabhushan, and M. Hale. 2008. Benefits and challenges of over-actuated excitation systems. *Proceedings of the 79th Shock and Vibration Symposium*. Arvonia, VA: SAVIAC.
2. Underwood, M. A. and T. Keller. 2006. Applying coordinate transformations to multi-DOF shaker control. *Sound and Vibration* (January 2006): 22–7.
3. Fitcher, E. F. 1986. A Stewart platform-based manipulator: General theory and practical considerations. *The International Journal of Robotics Research* 5 (2): 157–82.
4. Hunt, K. H. 1978. *Kinematic geometry of mechanisms*. Oxford, UK: Oxford University Press.
5. US Department of Defense. 2008. *MIL-STD-810G: Environmental engineering considerations and laboratory tests.* 527 Multi-Exciter Test. Washington, DC: US DOD.

ABOUT THE AUTHORS

Michael Hale is an electronics engineer and experimental developer in the Environmental Test Division of the Army's Redstone Test Center, US Army Developmental Test Command. He earned a BSEE from Auburn University in 1983 and his MSE and PhD degrees from the University of Alabama in Huntsville (UAH) in the Electrical and Computer Engineering Department in 1992 and 1998.

Norman Fitz-Coy is an associate professor in the Department of Mechanical and Aerospace Engineering at the University of Florida. He earned his PhD in Aerospace Engineering from Auburn University in 1990.

Contact author: Michael T. Hale, Redstone Test Center, Dynamic Test Division, Bldg. 7856, Redstone Arsenal, AL 35898-8052 USA.

---

electronics manufacturing and pharmaceutical processes; design, test, and evaluation of commercial and military equipment; and product reliability issues associated with commercial and military systems. IEST is an ANSI-accredited standards-developing organization. For more information about the many benefits of IEST membership, visit www.iest.org.